

## Characterization of Brazilian clay-supported triflic acid superacid catalysts by solid state $^{27}\text{Al}$ NMR

A. C. O. Silva, R. A. S. San Gil\*

Universidade Federal do Rio de Janeiro, Instituto de Química, Rio de Janeiro, Brazil  
rsangil@iq.ufrj.br

L. C. Dieguez

Universidade Federal do Rio de Janeiro, Nucat-COPPE, Rio de Janeiro, Brazil

**Keywords:** MAS NMR  $^{27}\text{Al}$ ; pillared clay; triflic acid

**Abstract:** In this communication, we report in the first time the characterization by solid state NMR of superacid sites generated by impregnation of Brazilian clay and  $\text{Al}_2\text{O}_3$ -pillared Brazilian clay with trifluoromethanesulfonic acid (TfOH). X-ray diffraction, textural and solid state  $^{27}\text{Al}$  NMR were used to characterize the catalysts. Four distinct  $\text{Al}^{\text{VI}}$  sites could be detected in  $^{27}\text{Al}$  MAS NMR spectra after treatment with TfOH and were assigned as: structural non-complexed Al, non-structural-OTf complexed Al, lamellar-OTf complexed Al and Al-pillared-OTf complexed Al resp.

**Resumo:** Esta comunicação apresenta a caracterização de sítios superácidos gerados em argilas brasileiras não pilarizadas e pilarizadas com  $\text{Al}_2\text{O}_3$  por impregnação com ácido trifluormetanossulfônico (TfOH). Foram empregadas as técnicas de difração de raios X, avaliação textural e RMN de  $^{27}\text{Al}$  no estado sólido para caracterização dos catalisadores. Quatro sítios distintos de AlVI puderam ser observados nos espectros de RMN MAS de  $^{27}\text{Al}$  após tratamento com TfOH e foram assinalados como: Al estrutural não complexado, Al não estrutural complexado com TfOH, Al estrutural (lamelar) complexado com TfOH e Al estrutural (pilares) complexado com TfOH, resp.

### Introduction

The constant search for more efficient catalytic processes has directed the research in this area with the use of solid acid possessing superacid characteristics, targeting more conversions and selectivities, with less steps and degree of environmental aggression. In the literature there are some examples of procedures of obtaining solid superacids.<sup>1-3</sup>

Following Henderson-Hasselbalch x Hammett e Deyrup,<sup>4</sup> superacid materials can be defined by  $H_0$  acidity function:



$$\text{pKa} = \text{pH} + \log ([\text{BH}^+]/[\text{B}])$$

$$\text{pKa} = H_0 + \log ([\text{BH}^+]/[\text{B}])$$

$$H_0 = \text{Hammett acidity function} = \text{pK}_{\text{BH}^+} - \log (c_{\text{BH}^+}/c_{\text{B}})$$

$c$  – molar concentration

Superacids present acid strength higher than 100%  $\text{H}_2\text{SO}_4$ , e.g.  $H_0 \leq -12$ . Mixture of Brønsted and Lewis acids also leads to superacid medium, as for example  $\text{HF-SbF}_5$  10% mol, with  $H_0 \sim -22$ . Trifluoromethanesulfonic acid, named triflic acid (TfOH) is a liquid with boiling point of 162 °C, that presents  $H_0 = -14.1$ .<sup>5</sup> It can be used for a catalyst in different chemical processes: alcohol dehydration,<sup>6</sup> aromatic alkylations<sup>7</sup> and oxidations.<sup>8</sup>

The work currently under development in our laboratory involves the use of Brazilian natural

clays as a source for preparation of catalysts with acid properties. After purification, the clay is treated with a solution containing metal complexes, as the  $Zr_4$  tetramer or the Keggin type aluminum complex,<sup>9</sup> named  $Al_{13}$  (Figure 1), followed by calcination, to generate metal-

pillared clays. This type of catalyst contains mostly Lewis acid sites located in the pillar region. There are in the literature some examples of the use of triflic acid to increase acidity of solid catalysts.<sup>10,11</sup>

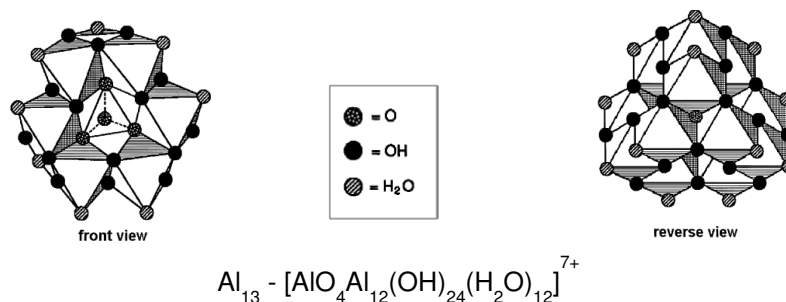


**Figure 1.**  $Al_{13}$  complex.

The objective of this work is to generate superacid clay catalysts through treatment with triflic acid. Solid state NMR observing  $^{27}Al$  is used as a probe to address the sites generated after reaction with  $TfOH$ . Also, X-ray diffraction and BET specific area (adsorption and desorption of liquid  $N_2$ ) measurements were used as complementary characterization techniques.

### Experimental

The clay sample used in this work is a smectite from the region of Campina Grande (PB) named Chocolate, with cation exchange capacity - CEC = 102 meq/100 g. The raw material was purified following procedure described in the literature.<sup>12</sup> The purified clay

was treated with  $Al_{13}$  solution obtained by hydrolysis of a basic solution  $AlCl_3 \cdot 6H_2O$  with  $NaOH$ .<sup>9</sup> The pillared clay was obtained after thermal treatment in the range of 473 to 673K. Two different  $TfOH$  treated samples were manufactured, hereafter designated purified clay/ $TfOH$  and  $Al$ -pillared clay/ $TfOH$ . They were made by mixing pure  $TfOH$  (Fluka, 98%) 10 times the CEC with clay sample in a glove box, under dry nitrogen atmosphere. The excess of acid was extracted with hexane. The catalysts prepared were maintained in a dry nitrogen atmosphere.

$^{27}Al$  solid state MAS NMR spectra were obtained on a Bruker Avance DRX300 (7.05 T) spectrometer operating at 78.5 MHz, with a 4mm MAS probe spinning the samples at 10 kHz. The samples were prepared by transferring the clay

to 4mm ZrO<sub>2</sub> rotors inside the glove box. All NMR spectra were recorded using a one-pulse sequence. The pulse width used was 1 $\mu$ s (tip angle  $\pi/12$ ). The recycle delay was set to 0.5 s. The spectra were referenced using an external sample of AlCl<sub>3</sub>.6H<sub>2</sub>O (0 ppm).

## Results and Discussion

The results of X ray diffraction, obtained for the catalysts are depicted in Table 1. It can be seen the principal diffraction peaks related with d<sub>001</sub> plane of lamellar material (basal spacing values) at around  $2\theta = 13 \text{ \AA}$ . Modification of this value to 16  $\text{\AA}$  after intercalation and pillarization is a good indication that a pillared structure was

achieved. After treatment with TfOH the purified clay and Al-pillared clay showed absence of d<sub>001</sub> plane, indicating formation of non crystalline materials.

Textural results (Table 1) showed an increase in the area from 76 m<sup>2</sup>.g<sup>-1</sup> to 278 m<sup>2</sup>.g<sup>-1</sup> after pillarization and confirms the formation of galleries inside the clay structure. Beside the increase in total area, it was obtained a material with higher amount of micropore structure, compared with the raw clay. After TfOH treatment the specific area become negligible, suggesting that TfOH occupied the interlamellar and microporous spaces and/or promoted the aggregation of the clay particles.

**Table 1.** Textural results obtained for the catalysts prepared.

sample	DRX d <sub>001</sub> (Å)	S <sub>BET</sub> (m <sup>2</sup> /g)	S <sub>micro</sub> (m <sup>2</sup> /g)	V <sub>Tot</sub> (cm <sup>3</sup> /g)	V <sub>micro</sub> (cm <sup>3</sup> /g)	V <sub>micro</sub> /V <sub>tot</sub> (%)
Purified clay	13	76	24	0.144	0.011	8
Purif. Clay/TfOH	n.d.	12	-	0.03	-	-
Al-pillared clay	16	278	223	0.213	0.104	49
Al-pill.clay/TfOH	n.d.	1	-	0.02	-	-

n.d.: not detected.

Figure 2 shows the spectra of <sup>27</sup>Al obtained for samples of purified and Al-pillared clay, for comparison. The spectrum of purified clay is dominated by the peak at 2 ppm, typical for montmorillonite<sup>9</sup> and corresponding to a well defined sixfold coordinated aluminium environment, and a small signal at around 70 ppm, probably due to tetrahedral substitution on

the clay structure in low concentration. In the other side in the spectrum of the pillared clay, besides the signal at 2 ppm it could be clearly seen that the peak corresponding to Al<sup>IV</sup> sites is more intense, due to the presence of Al<sub>2</sub>O<sub>3</sub> from pillars, thus confirming the results obtained by XRD and specific area.

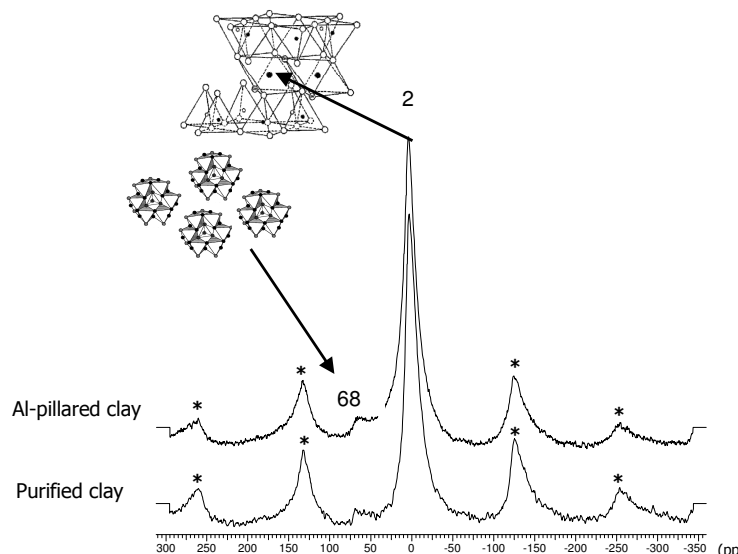


**Figure 2.**  $^{27}\text{Al}$  MAS NMR spectra of purified clay and Al-pillared clay. (\*) denotes spinning sidebands.

In the spectra of the samples treated with TfOH (Figure 3), the signal between 60 and 70 ppm corresponding to fourfold coordination aluminium sites ( $\text{Al}^{\text{IV}}$ ), present in the purified material (Figure 3, entry A) and in the Al-pillared clay (Figure 3, entry C), clearly disappeared (Figure 3, entries B and D resp.), and new signals were observed in the region of sixfold coordination aluminium sites ( $\text{Al}^{\text{VI}}$ ). It can be also seen by deconvolution of the spectrum of Al-pillared clay treated with excess of TfOH (Figure 3, entry D) the presence of four distinguishable peaks at shifts of -9 ppm, -2 ppm, 0.6 ppm and 3 ppm that correspond to  $\text{Al}^{\text{VI}}$  environments at all. The Al-pillared clay/TfOH sample was washed and dried, to remove excess of acid and soluble phases. In the  $^{27}\text{Al}$  MAS NMR spectrum of this sample (Figure 3, entry E) was observed a drastic reduction of the signal at around 0.6 ppm, suggesting that it corresponds to non structural

Al complexes with TfOH. The signal at -9 ppm could be assigned as corresponding to Al present in the pillar structure, complexes with TfOH. Finally the nature of the signal at -2 ppm was addressed by treating the purified clay sample with excess of TfOH. The  $^{27}\text{Al}$  MAS NMR spectrum obtained for this sample (Figure 3, entry B) presents only one signal at -2 ppm, indicating that this signal corresponds to  $\text{Al}^{\text{VI}}$  of the clay lamellar structure complexes with TfOH (Table 2).

According to Fyfe<sup>13</sup> the signal width of a quadrupolar nucleus depends on the central quadrupolar constant ( $C_Q$ ) and on the value of quadrupolar asymmetry factor ( $\eta_Q$ ). The peaks obtained for the samples treated with TfOH are somewhat narrow, corresponding to the presence of ordered crystalline phases generated by interaction of Al sites with TfOH and indicating a relatively small  $C_Q$  distribution. It

is proposed that signals in the negative range of the scale correspond to the sites of  $\text{Al}^{\text{IV}}$  and  $\text{Al}^{\text{VI}}$  from purified and Al-pillared clays complexes

with TfOH molecules, respectively. Further experiments are in progress to confirm this suggestion.

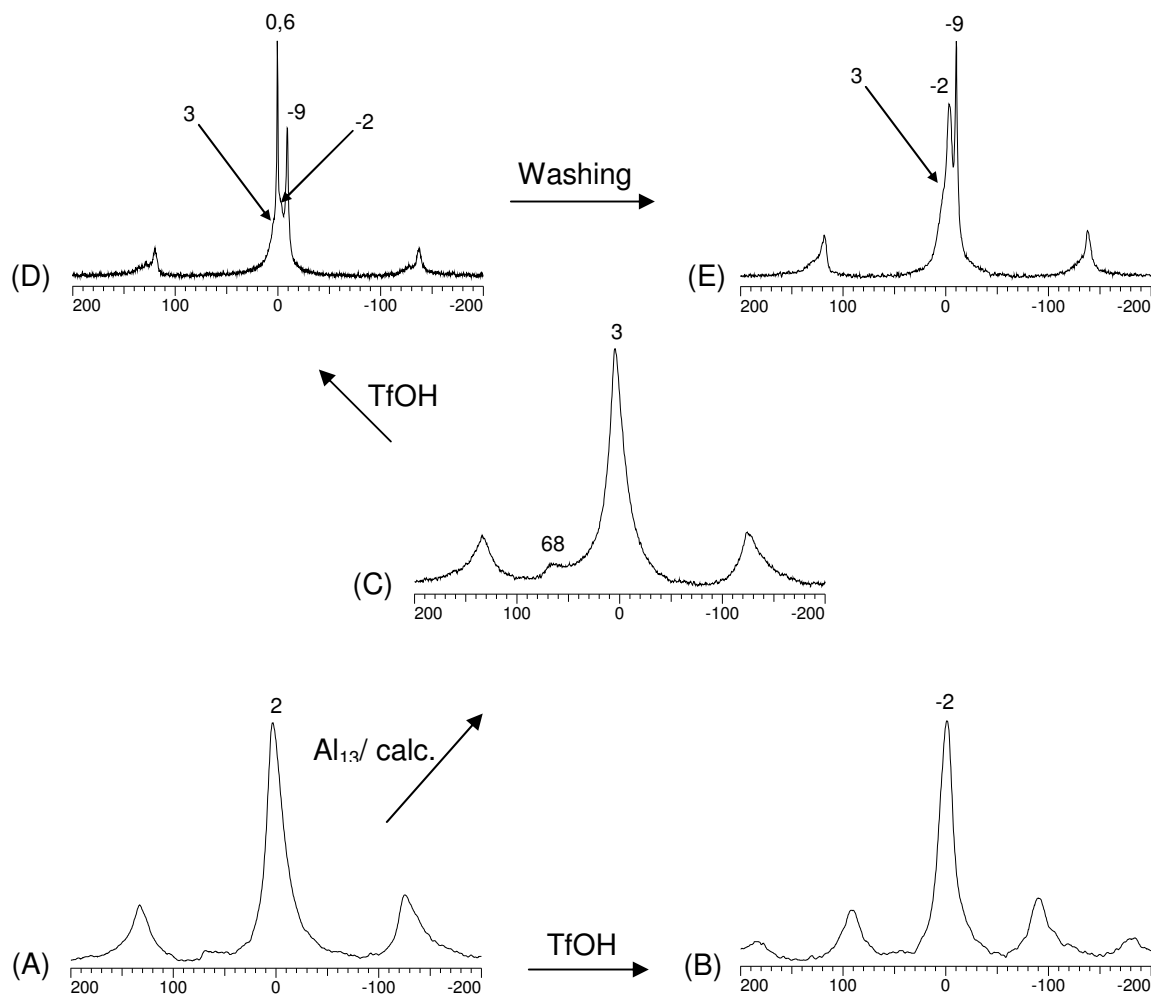


**Figure 3.** Solid state  $^{27}\text{Al}$  MAS spectra obtained for (A) purified clay; (B) purified clay treated with excess of triflic acid; (C) Al-pillared clay obtained from purified clay after intercalation with  $\text{Al}_{13}$  complex and calcination; (D) Al-pillared clay after treatment with triflic acid; (E) spectrum obtained for sample D, after washing. Except spectrum B, obtained under 7KHz the spectra were obtained with spinning rate of 10 KHz.

**Table 2.** Data obtained from the  $^{27}\text{Al}$  MAS NMR spectra.

sample	$\delta$ , ppm		Assignment proposed
Purified clay	2	$\text{Al}^{\text{VI}}$	lamellar structure
		$\text{Al}^{\text{IV}}$	lamellar structure
Purified clay/TfOH <sub>exc.</sub>	-2	$\text{Al}^{\text{VI}}\text{-OTf}$	lamellar structure
Al-pillared clay	3	$\text{Al}^{\text{VI}}$	lamellar structure+ $\text{Al}_2\text{O}_3$ pillar
	68	$\text{Al}^{\text{IV}}$	$\text{Al}_2\text{O}_3$ pillar structure
Al-pillared clay/TfOH	3	$\text{Al}^{\text{VI}}$	lamellar structure
	0.6	$\text{Al}^{\text{VI}}\text{-OTf}$	non-lamellar species
	-2	$\text{Al}^{\text{VI}}\text{-OTf}$	lamellar structure
	-9	$\text{Al}^{\text{VI}}\text{-OTf}$	$\text{Al}_2\text{O}_3$ pillar structure
Al-pillared clay/TfOH/after washing	3	$\text{Al}^{\text{VI}}$	lamellar structure
	-2	$\text{Al}^{\text{VI}}\text{-OTf}$	lamellar structure
	-9	$\text{Al}^{\text{VI}}\text{-OTf}$	$\text{Al}_2\text{O}_3$ pillar structure

## Conclusion

This communication reports for the first time in the literature the characterization of superacid clay derived catalysts, obtained from Brazilian pillared clay treated with triflic acid by using solid state  $^{27}\text{Al}$  NMR spectroscopy. Although XRD indicate that no crystalline catalysts are generated, maybe due to small particle sizes that broadened the XRD peaks, three distinct aluminium sites have been observed using  $^{27}\text{Al}$  MAS NMR. This is one of the advantages of NMR over XRD in investigating materials with small crystalline sizes, as is the case of clay-based catalysts.

## Acknowledgements

The authors acknowledge the financial support from CAPES (scholarship A.C.O. Silva).

## References

1. A. de Angelis, C. Flego, P. Ingallina, L. Montanari, M. G. Clerici, C. Carati, C. Perego, *Catal. Today* **65** (2001) 363.
2. T. Benson, R. Hernandez, T. French, E. Alley, W. Holmes, *J. Mol. Catal. A: Chemical* **274** (2007) 173.
3. A.N. Parvulescu, B. C. Gagea, V. I. Parvulescu, D. De Vos, P. A. Jacobs, *Appl. Catal. A: General* **306** (2006) 159.
4. L.P. Hammett, A.J. Deyrup, *J. Am. Chem. Soc.* **54** (1932) 2721.
5. L.K. Noda, *Quimica Nova* **19** (1996) 135.
6. O. Macias, J. Largo, C. Pesquera, C. Blanco, F. Gonzalez, *Applied Catalysis, A: General* **314** (2006) 23.
7. B. N. Narayanan, S. Sugunan, *Reaction Kinetics and Catalysis Letters* **89** (2006) 45.
8. S. Zuo, R. Zhou, *Applied Surface Science* **253** (2006) 2508.

9. S.Q.M. Leite, L.C. Dieguez, S.M.C. Menezes, R.A.S. San Gil, *Química Nova* **23** (2000) 149.
10. M.C. Al-Kinary, B.Y. Jibril, S.H. Al-Khowaiter, M.A. Al-Dosari, H.A. Al-Megren, S.M. Al-Zahrani, K.I. Al-Humaizi, *Chemical Engineering and Processing* **44** (2005) 841.
11. D.O. Bennardi, G.P. Romanelli, J.C. Autino, L.R. Pizzio, *Applied Catal.A:general* **324** (2007) 62.
12. I.B. Aranha, C.H. Oliveira, R. Neumann, A. Alcover Neto, P. Munayco, R.B. Scorzelli, R.A.S. San Gil, *Arquivos do Museu Nacional* **65** (2007) 1.
13. C. A. Fyfe, *Solid State NMR for Chemists*, C.F.C. Press, Ontario, 1983.